# Supplementary Information

# Thermo-resistive and thermo-piezoresistive sensitivity of carbon nanostructure engineered thermoplastic composites processed via additive manufacturing

Pawan Verma[a], Andreas Schiffer[b], S. Kumar[c*]

[a]Artie McFerrin Department of Chemical Engineering, Texas A&M University, College Station, TX 77840

[b]Department of Mechanical Engineering, Khalifa University of Science and Technology, 127788, Abu Dhabi, United Arab Emirates

[c]James Watt School of Engineering, University of Glasgow, Glasgow, G12 8LT, UK

[*] Corresponding author: s.kumar@eng.oxon.org

## S1. Differential Scanning Calorimetry (DSC)

For the DSC analysis, a Perkin-Elmer Pyris 6 was used in $N_2$ atmosphere. First, the sample was heated from room temperature to 180 °C and then held for 2 min to remove the thermal history of the polymer. Then, the sample was cooled to room temperature and then again heated up to 180 °C. The heating and cooling rates (10 °C/min) were kept constant in all cycles and about 10 mg of sample weight was used for recording DSC scans.

In the cooling scan, an exothermic transition due to crystallization was observed in all the samples, as seen from Fig. S1a. The results also showed that the addition of MWCNTs to the PPR resulted in a marginal increase in crystallization onset temperature, $T_{onset}$, and peak exotherm temperature, $T_c$. The increase in $T_c$ confirms the nucleating effect of the MWCNTs.

The results obtained from the second heating scans are presented in Fig. S1b, showing two melting endotherms for each sample, which are observed here due to previous crystallization conditions (cooling rate) or melting of lamellar crystals of different sizes. The endothermic peak temperatures, denoted as $T_{m1}$ and $T_{m2}$, respectively, did not show any significant changes upon incorporation of varying contents of MWCNTs while the observed decrease in the onset of melting confirms the formation of imperfect crystals in the presence of MWCNTs [1]

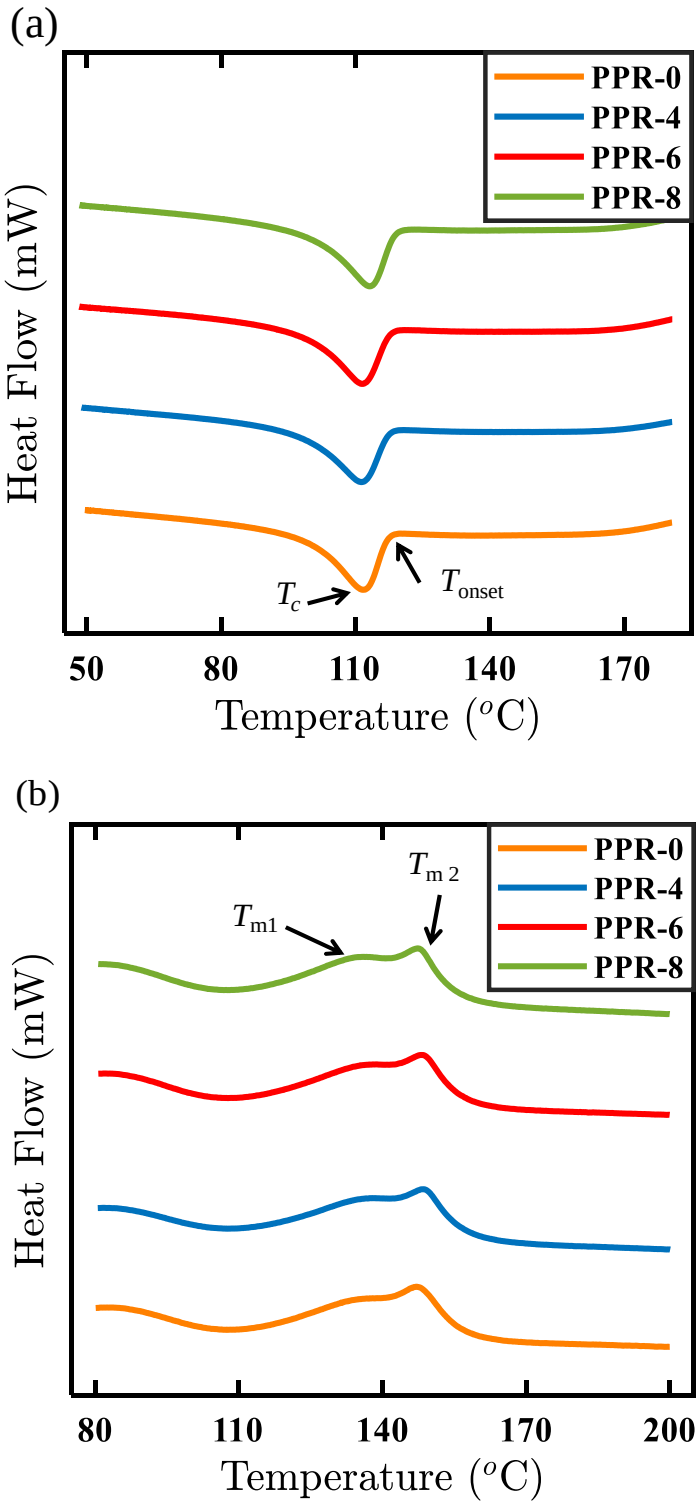


**Fig. S1** DSC thermographs showing crystallization (a) cooling and (b) heating scans of PPR and MWCNT/PPR composites.

## S2. Supporting data

**Table S1.** TCR and temperature ranges of polymer-based nanocomposites reported in the literature and in this study.

| No | Composite | Temperature (°C) | TCR ($10^6$/°C) | Ref |
|---|---|---|---|---|
| 1 | CNT/vinyl ester | 40 – 160 | -1.2 … +2,400 | 51 |
| 2 | MWCNT/PSF | 25 – 100 | -3,040 … +4,140 | 53 |
| 3 | CNT/glue/paper | 20-75 | -2,400 | 54 |
| 4 | CNT/PEEK | 20-140 | -7,580 | 55 |
| 5 | MWCNT/SEBS | 20-60 | -3,710 | 56 |
| 6 | CNT-based thermistor | 25-65 | -7,950 … -2,130 | 65 |
| 7 | 3D-printed PPR/MWCNT | 30-100 | -11,820 … -6,670 | this work |

**Table S2.** Gauge factors and strain ranges of polymer-based nanocomposites reported in the literature and in this study.

| No | Composite | Temperature (°C) | Strain range (%) | Gauge factor | Ref. |
|---|---|---|---|---|---|
| 1 | CB/PDMS | RT | < 80 | 1.8-5.5 | 78 |
| 2 | CNT/PDMS | RT | < 10 | 4.36 | 79 |
| 3 | CB/PDMS | RT | < 10 | 15.75 | 79 |
| 4 | CNT-CB/PDMS | RT | < 300 | 0.91-13.1 | 80 |
| 5 | CNT/PDMS | RT | < 45 | 35.75 | 81 |
| 6 | SWCNT/Porous PDMS | RT | < 160 | 24-134 | 82 |
| 7 | MWCNT/PDMS | RT | < 9 | 1140 | 83 |
| 8 | CNS/PDMS | RT | < 110 | 8-47 | 49 |
| 9 | MWCNT/TPU | RT | < 100 | 2.0-6423 | 84 |
| 10 | CF/PDMS yarn | RT | < 5 | <700 | 85 |
| 11 | CNT/SBS fiber | RT | < 267 | <2889 | 86 |
| 12 | CNF/porous PDMS | RT | < 70 | 1-6.5 | 87 |
| 13 | Graphene foam/PDMS | RT | < 3 | 120 | 7 |
| 14 | 3D-printed PPR/MWCNT | 30 | 0-8 | 17.1-27.8 | this work |
| 15 | 3D-printed PPR/MWCNT | 60 | 0-20 | 52.3-395 | |
| 16 | 3D-printed PPR/MWCNT | 100 | 0-100 | 6.6-9.0 | |

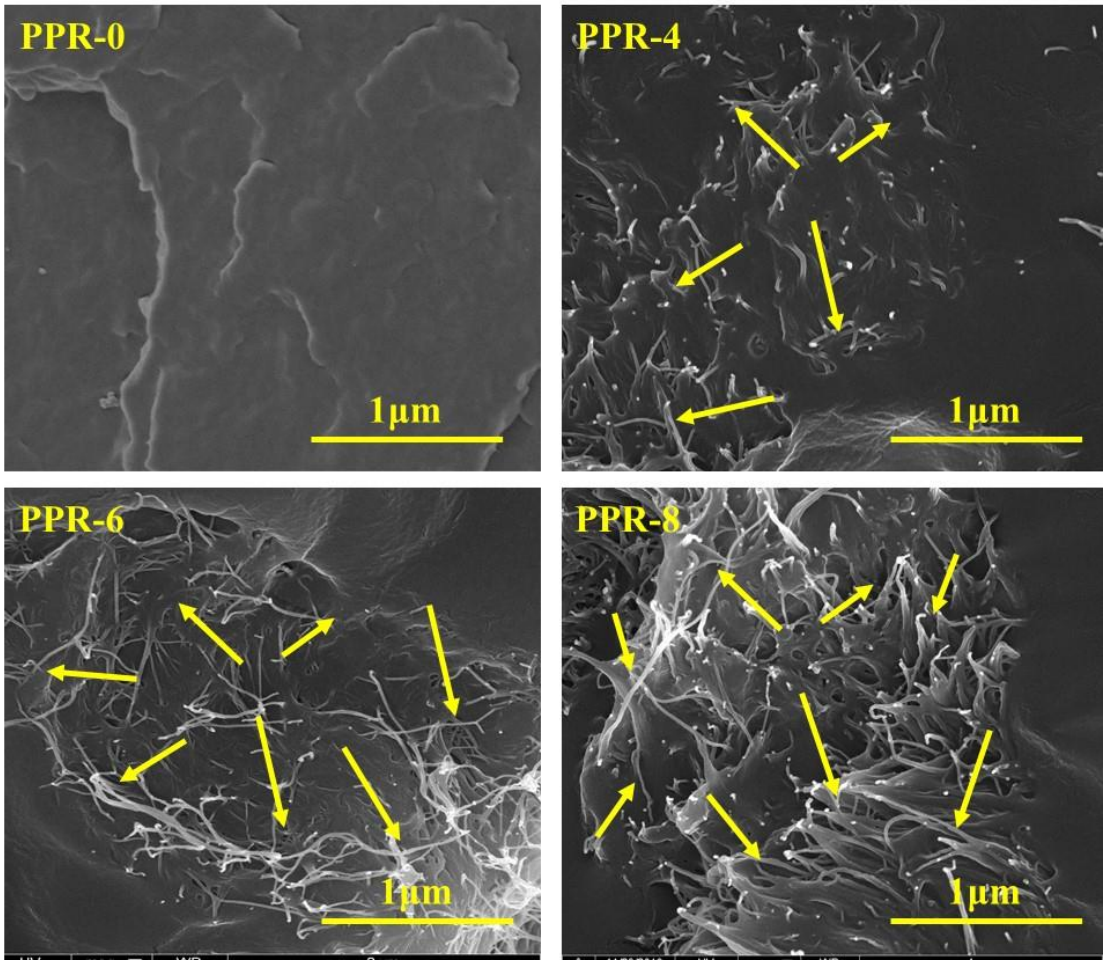


**Fig. S2.** SEM micrographs of MWCNT/PPR composites with varying MWCNT loading (yellow arrows indicate the MWCNT dispersion in PPR matrix).

The surface morphology of the cryogenically fractured surface of MWCNT/PPR composites were analyzed using Nova Nano SEM 50 series, operated at 10 kV to examine the state of dispersion within the PPR matrix, as shown in Fig. S2.

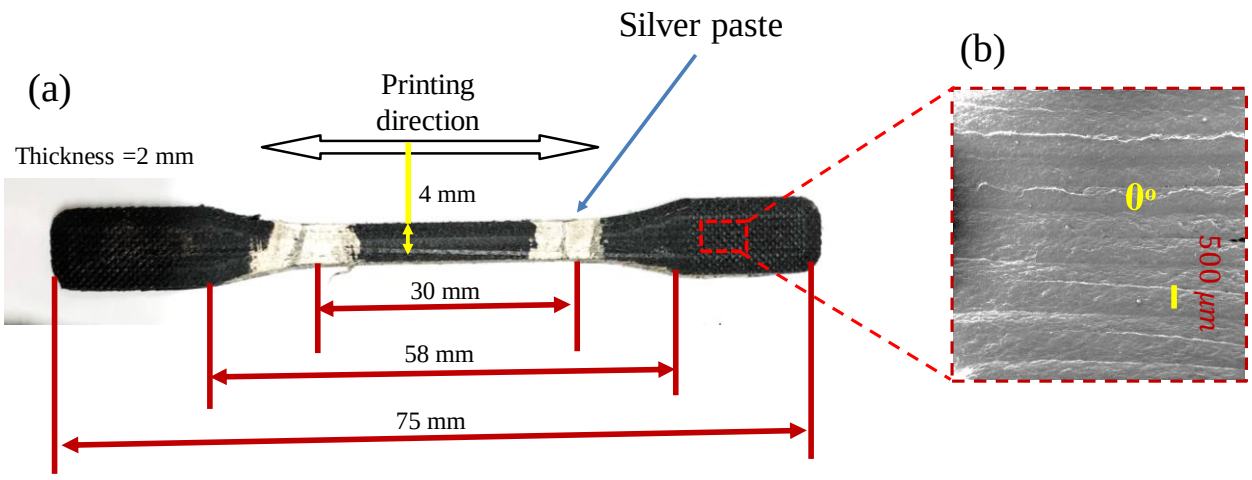


**Fig. S3** (a) Photograph of 3D printed MWCNT/PPR specimen according to ISO 527; (b) SEM images of sample displaying printing direction.

## References

S1. Verma P, Choudhary V. Polypropylene random copolymer/MWCNT nanocomposites: Isothermal crystallization kinetics, structural, and morphological interpretations. Journal of Applied Polymer Science. 2015;132(13):n/a-n/a.